Received: 13 November 2022 | Revised: 7 May 2023 | Accepted: 28 May 2023

DOI: 10.1002/jsp2.1267

RESEARCH ARTICLE

JOR Spine OPEN ACCESS

The influence of intervertebral disc overloading on nociceptor calcium flickering

Jan Gewiess[1,2] | Janick Eglauf[1] | Astrid Soubrier[1] | Sibylle Grad[1] | Mauro Alini[1] | Marianna Peroglio[3] | Junxuan Ma[1]

[1]AO Research Institute, AO Foundation, Davos, Switzerland

[2]Department of Orthopaedic Surgery and Traumatology, Inselspital, Bern University Hospital, University of Bern, Bern, Switzerland

[3]École des Mines de Saint-Étienne, Univ. Lyon, Saint-Etienne, France

Correspondence
Junxuan Ma, AO Research Institute Davos, Clavadelerstrasse 8, 7270 Davos Platz, Switzerland.
Email: junxuan.ma@aofoundation.org

Funding information
AO Foundation

Abstract

Introduction: Mechanical overloading can trigger a degenerative-like cascade in an organ culture of intervertebral disc (IVD). Whether the overloaded IVD can influence the activation of nociceptors (i.e., the damage sensing neurons) remains unknown. The study aims to investigate the influence of overloaded IVD conditioned medium (CM) on the activation of nociceptors.

Methods: In the static loading regime, force-controlled loading of 0.2 MPa for 20 h/day representing "long-term sitting and standing" was compared with a displacement-controlled loading maintaining original IVD height. In the dynamic loading regime, high-frequency-intensity loading representing degenerative "wear and tear" was compared with a lower-frequency-intensity loading. CM of differently loaded IVDs were collected to stimulate the primary bovine dorsal root ganglion (DRG) cultures. Calcium imaging (Fluo-4) and calcitonin gene-related peptide (CGRP) immunofluorescent labeling were jointly used to record the calcium flickering in CGRP(+) nociceptors.

Results: Force-controlled loading led to a higher IVD cell death compared to displacement-controlled loading. Both static and dynamic overloading (force-controlled and high-frequency-intensity loadings) elevated the frequency of calcium flickering in the subsurface space of CGRP(+) nociceptors compared to their mild loading counterparts.

Conclusion: In the organ culture system, IVD overloading mediated an altered IVD-nociceptor communication suggesting a biological mechanism associated with discogenic pain.

KEYWORDS
calcium imaging, dorsal root ganglion, intervertebral disc, organ culture

1 | INTRODUCTION

Low back pain (LBP) is the leading cause of disability worldwide.[1] The intervertebral disc (IVD) is the most frequent pain generator (~40%).[2] Severity of IVD degeneration correlates with chronic LBP prevalence.[2] Understanding the communicating mechanism between IVD and sensory nervous system in chronic LBP may help to discover new preventive and therapeutic approaches.

Among multiple factors, spinal overloading is frequently discussed as a potential risk factor of chronic LBP.[3–5] Nevertheless, the exact role of mechanical loading on chronic LBP is not determined. Measuring spinal loading in vivo is challenging. Several clinical studies aimed to investigate the influence of IVD loading on LBP.[3–5] However, they generally evaluate IVD loading using questionnaires based on "occupational exposures," "exercise," and "sitting time" and so on, which are prone to subjective bias and low accuracy.[5]

In this context, IVD organ culture systems have been developed to study the influence of mechanical loadings on IVD degeneration.[6] In the organ culture system, the IVD loading can be controlled and monitored.[6] Using the organ culture system, the effects of both static and dynamic loadings on IVD cell death, matrix homeostasis and pro-inflammatory gene expression have been well-established.[7] Nevertheless, current organ culture systems do not include the pain-mediating neural compartments. Whether the loading-induced IVD degeneration correlates with pain-associated neural activation remains unclear.

In the peripheral sensory nervous system, the nociceptors (i.e., the damage sensing neuronal subtype in the dorsal root ganglion (DRG)[8]) are the first order neurons that sense pain signals and are essential contributors of chronic pain.[9] Blocking the nociceptors peripherally can relief chronic pain in humans.[10] Nerve fibers from the nociceptors expressing calcitonin gene related peptide (CGRP) are found to grow into deeper regions of the IVD in chronic LBP patients.[11,12] The ectopic discharges of these nociceptors (i.e., the firing of the nociceptors in the absence of noxious stimuli) are correlated to spontaneous and ongoing pain.[13]

Calcium imaging is a useful tool to characterize the ectopic discharges of nociceptors.[14] An earlier study simultaneously used patch-clamp and calcium imaging to evaluate neuronal discharge. They found the calcium flickering in neurons were in synergy with the ectopic action potential discharges.[15] The calcium flickering in the subsurface space of DRG neuronal soma (cell body) has been proved to arise from the "calcium induced calcium release" mechanism which is coupled to the neuronal discharge-induced calcium influx.[16] This calcium flickering in nociceptors is also responsible for pain-related neurotransmitter release.[16]

We hypothesize that the conditioned medium of overloaded IVD can elevate the calcium flickering of nociceptors. We evaluated the effects of two types of overloading (static[17] and dynamic[18]) which were compared to their corresponding mild loading controls, respectively. Conditioned media (CM) of these differently loaded IVD were applied to stimulate the bovine primary DRG cell culture. We performed CGRP immunofluorescent labeling following the calcium imaging in the DRG cell culture. In this way, the CGRP(+) nociceptors could be distinguished from multiple DRG cell types and the calcium flickering in the CGRP(+) nociceptors could be exclusively analyzed.

2 | MATERIALS AND METHODS

2.1 | General study design

The study design is presented in Figure 1:

1. In the static loading regime, FC (force-controlled group) representing "long-term sitting and standing" associated overloading was compared with DC (displacement-controlled group) control (Figure 1A,B). In the FC group, a constant compressive loading of 0.2 MPa was applied to the IVDs. In the DC control group, a displacement-controlled loading was applied to maintain the original IVD height (measured immediately after dissection). Both FC and DC loadings were 20 h/day over seven consecutive days (Figure 1B).
2. In the dynamic loading regime, DL (degenerative loading) representing "wear and tear" associated overloading was compared with PL (physiological loading) control (Figure 1C,D). In the DL group, a high-frequency-intensity sinusoidal dynamic loading (0.38–0.42 MPa, 5 Hz) was applied to the IVDs. In the control PL group, a lower-frequency-intensity loading (0.02–0.2 MPa, 0.2 Hz) was applied. Both PL and DL loadings lasted for 3 h/day over five consecutive days (Figure 1D).

Our hypothesis is that the overloaded IVD may stimulate the nociceptors in DRG proximal to the IVD and increase their ectopic discharge[13] (Figure 1E) This was modeled by using the overloaded IVD CM to stimulate primary bovine DRG cell culture. Ectopic discharge associated calcium flickering in subsurface space of neurons was recorded using calcium imaging. Among the multiple cell/neuron types in the DRG, the nociceptors were identified using CGRP immunofluorescent labeling following calcium imaging recording (Figure 1F).

2.2 | IVD loading in the organ culture model

Bovine tails (age 4–6 months) were obtained from a local abattoir, whereby no animal was intentionally sacrificed for our study. Six bovine donors (six tails) were included for the static loading study. Two to four IVDs per tail were harvested at the location 5–8 segments from the distal end of the tail. These two to four IVDs from the same tail were assigned to DC and FC groups, respectively. Four bovine donors (four tails) were used for dynamic loading study. Two IVDs from each tail were assigned to PL and DL groups, respectively. Group assignment was performed to ensure the equality of IVD sizes between groups (diameters of IVDs ranged from 6 to 12 mm; heights of IVDs ranged from 6 to 11 mm).

The IVDs were dissected by cutting through the cartilage growth plate within a motion segment using a scalpel and a plier. The two endplates of each IVD were trimmed to ensure parallelism. Blood clots in the endplates were removed using a jet lavage system. The IVD height was immediately measured after dissection. Then, the IVDs were sequentially rinsed in phosphate buffered saline (PBS) containing 10% penicillin–streptomycin (PS, 15140-122, Gibco, UK) and PBS with 1% PS. IVDs were cultured in 4.5 g/L glucose Dulbecco's Modified Eagle Medium (DMEM, 52100-021, Gibco, Paisley, UK) containing 10% fetal calf serum (FCS, 35-010-CV, Corning, CA, USA), 1% PS, 0.11 g/L sodium pyruvate (P5280; Sigma-Aldrich, JP), 20 mM HEPES

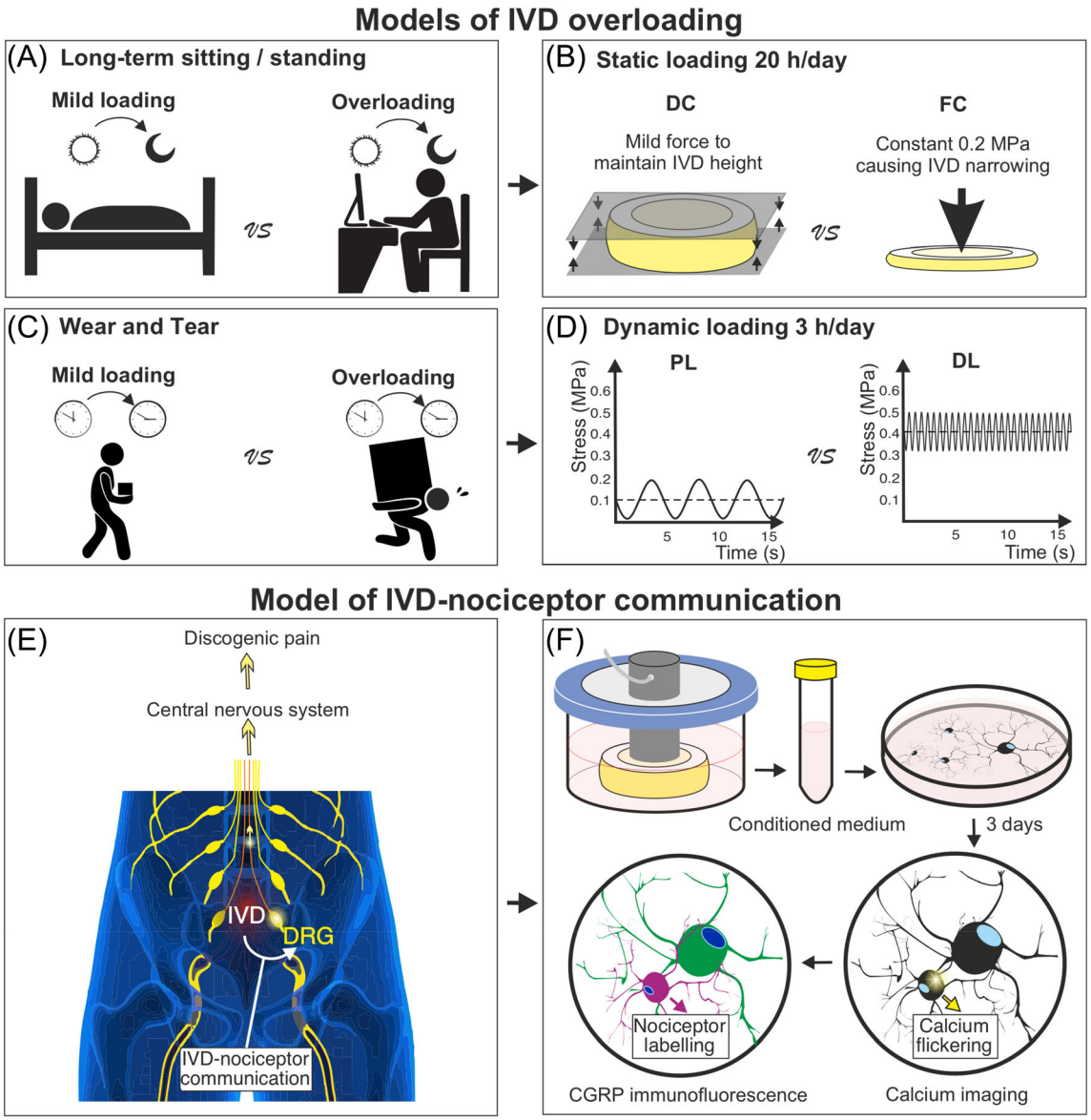

FIGURE 1 Schematic of the study hypothesis and design. Daily activity associated IVD loadings (mild loading versus overloading) (A,C) were modeled in the organ culture of IVD (B,D). (E) Overloaded IVD is hypothesized to communicate with nociceptors in DRG causing elevated pain/nociceptive signals in the nociceptors. (F) In the model, overloaded IVD conditioned media were used to stimulate nociceptors. Calcium flickering in these CGRP(+) nociceptors was investigated in vitro. DC, displacement-controlled loading; DL, degenerative dynamic loading; FC, force-controlled loading; PL, physiological dynamic loading.

(15 630 122, Thermo Fisher, USA), 1% ITS universal culture supplement (354352, Sigma-Aldrich, MO, USA) and 0.2% Primocin (ant-pm, InvivoGen, San Diego, CA, USA). The loading was initiated in a custom-designed bioreactor system[7] after overnight free-swelling culture in 6 well-plates at 37°C, 90% humidity and 5% CO_2. Force and deformity were real-time monitored using sensors in the bioreactor. Data recording frequency was 10 Hz. An algorithm in DSPACE was designed to control the regimes of IVD loading.

In the static loading regime, a compressive pressure of 0.2 MPa was applied to the IVDs 20 h/day for 7 days in the FC group. In the DC control group, IVDs were maintained in the bioreactor keeping the original IVD height (measured immediately after dissection) also 20 h/day. The IVDs were maintained in free swelling condition for 4 h when performing the medium change, IVD measurement and bioreactor setup.

In the dynamic loading regime, high-frequency-intensity loading (sinusoidal loading ranging from 0.38 to 0.42 MPa at 5 Hz for 3 h/day) was applied to the IVDs for 5 days (degenerative dynamic loading, DL) based on a formerly described protocol.[19] As the control, a sinusoidal loading between 0.02 and 0.2 MPa at 0.2 Hz was applied for 3 h/day for 5 days (physiological dynamic loading, PL). During these 3 h of loading, IVDs were kept in the loading chamber with 4 mL medium taken from a 30 mL medium pool. After loading, the IVDs and the 4 mL medium were transferred to a larger culture chamber containing this 30 mL medium and maintained in free-swelling condition.

2.3 | IVD conditioned medium collection

The CM were collected at day 5 for both static and dynamic loading studies to stimulate nociceptors because former proteomic study showed that more than 100 cytokines are upregulated in the over-loaded IVD CM compared to mildly loaded IVD CM between day 4 and 6.[19] One IVD per donor was used to generate CM in each group. CM coming from different donors were not pooled and represented the biological replicates. The CM of static/dynamic loaded IVDs were stored at −80°C before use.

For the static loadings (DC vs. FC), the IVDs were maintained in the loading chambers for 20 h. The loading chamber only allowed to contain 4 mL medium. Thus, daily medium change was performed to ensure IVD survival. Since only 4 mL CM per IVD was collected at day 5, 3 out of the 6 IVD donors were used to stimulate nociceptors. CM from the other 3 IVD donors were used in a pilot study.

For dynamic loadings (PL vs. DL), the IVDs were mostly kept outside the loading chamber in a larger amount of medium (in 30 mL medium for 21 h/day), there was no need to change the medium every day as in the static loading counterpart. A change of this 30 mL medium for each IVD was performed after 3 days. Also, a larger amount of CM was collected from each IVD and there were enough CM for all the four IVD donors.

The IVD conditioning of the media lasted shorter for static loading (24 h due to medium change every day) compared to dynamic loading (48 h from medium change at day 3 to CM collected at day 5). Also, the volumes of the static loaded IVD CM (4 mL) were smaller than dynamic loaded IVD CM (30 mL). Static and dynamic loading studies may have different concentrations of IVD secreted factors and are thus not comparable in terms of the CM's influence on nociceptors. Instead, our aim was to compare DC versus FC (static loading) and to compare PL versus DL (dynamic loading), while static and dynamic loadings were two separate and independent studies.

2.4 | Lactate dehydrogenase staining for IVD cell viability analysis

After loading, one IVD per group was snap frozen in cryo-compound (Tissue-Tek, O.C.T.™, Sismex, Horgen, CH) after removing cartilaginous endplate from one side of the IVD. Cryosections of 10 µm thickness were obtained using a microtome (HM 500 OMV, DE). Lactate dehydrogenase (LDH) staining is a popular method to evaluate musculoskeletal tissue viability. The purple staining under transmitted light depends on the activity of LDH in living cells which can be preserved when tissue is snap frozen. Dead cells loss the enzyme activity 36 h after cell death and is therefore not stained into the purple color, while their nuclei can be detected by ethidium homodimer-1 staining.[20]

LDH staining method was performed based on a formerly described protocol.[21] Briefly, the sections were firstly stained in a 40% polypep solution (P5115, Sigma, Buchs, CH) containing 54 mM lactic acid (69 771, Fluka, Buchs, CH) and 1.75 mg/mL β-nicotinamide adenine dinucleotide hydrate (43410, Fluka, Buchs, CH). Then, the sections were stained with 1 µg/mL ethidium homodimer-1 (46043, Sigma, DE). Imaging was performed using an upright optical microscope (Olympus BX63, Nikkei, JP). Under 20× magnification, LDH staining was imaged using the bright field channel, and ethidium homodimer-1 was imaged under the 528 nm excitation and 617 nm emission. Four to 8 images were taken at nucleus pulposus (NP), inner annulus fibrosus (iAF) and outer annulus fibrosus (oAF) regions. Living cells were stained by LDH, and dead cell nuclei were identified by ethidium homodimer-1 staining without surrounding purple LDH staining. IVD cell viability was defined as the proportion of living cells among all cells. Despite viability, degeneration associated gene expression in static loaded IVD was evaluated using quantitative-real-time-PCR. The methods and results were included in Supporting information.

2.5 | Adult bovine DRG cell culture

Adult bovine DRG cell culture was based on a formerly reported protocol.[22] Briefly, adult bovine DRGs (10–12-month-old) were obtained from cadaveric cervical spines (C 1–7) at a local abattoir. To dissociate cells from DRG tissue, DRGs were sliced and enzymatically digested in 4 mg/mL collagenase P (Roche, Mannheim, DE) on an orbital shaker for 3 h. Trituration of the loosened DRGs was performed using a P1000 pipette tip until the digested tissue pieces could easily pass through the pipette tip. The cell suspension was passed through a 100 µm cell strainer (Falcon, Corning, USA) to eliminate undigested tissue. The cell suspension was diluted in an equal amount of DMEM/F12 medium (50%, v/v, DMEM from Gibco, 52100-021, UK and F-12 Ham from Sigma, N6760, UK) supplemented with 10% FCS. Cells were separated from tissue debris by a "density gradient centrifugation" using 5 mL of 15% BSA in a 50 mL Falcon tube (the speed of centrifugation was 1800 rpm for 7 min). Cell pellet was resuspended in DMEM/F12 medium with 10% FCS. Cells were seeded at the density of 5000 neurons/cm^2 in 18-Well slide chambers (81816-IBI, Ibidi, DE). The culture medium was DMEM/F12 supplemented with 10% FCS, 1% penicillin/streptomycin, 0.44 g/L sodium pyruvate, 0.4 mM Ascorbic acid (84271, Sigma, MO, USA), 20 mM HEPES and 1% ITS. After 2 days of culture, the medium was changed to IVD CM. The CM stimulation of primary DRG cells lasted for 3 days. We chose 3 days for CM stimulation because of a glial over-proliferation in a longer DRG culture.[23] DRG cells from two bovine donors were included for both static and dynamic loading studies.

2.6 | Calcium imaging and immunofluorescence

The calcium imaging method was based on a formerly reported protocol.[24] Briefly, DRG cells were loaded with 5 µM Fluo-4-AM (ThermoFisher, F14201, USA), and calcium imaging was performed in Krebs–Ringer's solution (NaCl 119 mM, KCl 2.5 mM, NaH_2PO_4 1.0 mM, $CaCl_2$ 2.5 mM, $MgCl_2$ 1.3 mM, HEPES 20 mM and D-glucose 11.0 mM). Time-lapse images were acquired using a LSM800 confocal microscope (Zeiss, DE) at 10× magnification, 85 µm pinhole, 488 nm

excitation and 509 nm emission. The image acquisition rate was 1 Hz and the recording time was 110 s. The first 100 s were taken without any stimulus to study the spontaneous calcium flickering. To distinguish living neurons from dead ones, at the 100th second, 5 µL of 500 mM potassium chloride (KCl, final concentration at 50 mM) was added to the DRG cells. Only cells exhibiting immediate potassium-induced depolarization were considered as living neurons.

CGRP(+) nociceptors could be distinguished from other neuron populations in the calcium imaging analysis by a following Immunofluorescent labeling. The cells were immediately fixed in 4% formalin (Formafix, cat. n. 1803032, CH) after calcium imaging. For the immunofluorescence, the primary antibodies included rabbit anti-CGRP primary antibody (1:1000, 24 112, Immunostar, Sodiag Avegno, WI, USA) and mouse anti-neurofilament 200 (NF200) primary antibody (1:100, OMA1-06117, Thermo scientific, NL). The primary antibody incubation was at 4°C overnight. After washes, the cells were incubated with secondary antibody at room temperature for 1 h. The secondary antibodies included goat anti-mouse AlexaFluor 488 conjugated antibody (1:500, A-11029, Thermo Fisher, OR, USA) and donkey anti-rabbit AlexaFluor 680 conjugated antibody (1:500, A32802, Thermo Fisher). Nuclei were stained using Hoechst (1 µM, Sigma, cat. n. 14530, USA). Stained cells were imaged at an excitation wavelength of 470, 655, and 357 nm for NF200, CGRP and Hoechst staining, respectively, using EVOS™ FL Auto 2 Imaging System (Thermo Fisher Scientific). The neuronal soma was manually segmented using "Freehand Selection Tool" in ImageJ Fiji (version 1.52p, NIH, USA). The "Feret's diameter" (the longest distance between any two points along the selection boundary) of the neuronal somas were calculated.

The calcium imaging and the following immunofluorescent imaging were performed at the same location. This was achieved by taking notes of the calcium imaging location, that is, the distances between the calcium imaging field border and the culture well border. Living neurons identified in calcium imaging video were recognized in the immunofluorescent image using "Sync Windows" plugin in ImageJ Fiji. This allowed calcium signal analysis specifically in CGRP(+) nociceptors (Figure 2A–C).

Former study proved that calcium signals from the subsurface space of the cell bodies are coupled with discharge-related calcium influx.[16] Therefore, in our analysis, a squared region of Interest (ROI, pixel size 10 × 10) was manually defined at the subsurface space of nociceptor soma using the square selecting tool in ImageJ Fiji (version 1.52p, NIH, USA) (Figure 2D,E). The fluorescence change over time was quantified using "ROI manager" and "multi-measure function" within ImageJ Fiji.

A calcium peak was defined as a snap fluorescence increase followed by a fluorescence decay. To distinguish biologically relevant signals from background noise, we defined a threshold of calcium peak height based on the analysis of dead neuron fluorescent oscillations. Dead neurons were identified as neurons without a KCl-induced depolarization. The fluorescent oscillations of dead neurons were referred to as noise. By recording fluorescent oscillations of 21 dead neurons, we obtained a distribution of noise peak heights. Then, the threshold to subtract noise was defined as the upper border of 99% confident intervals of maximum noise peak heights among different cells (bootstrapping method). In living neurons, only calcium peaks higher than the threshold were regarded as biological relevant calcium signal for analysis (Figure 2F,G). Based on the bootstrapping estimation, the false positive probability of calcium signal detection was thus smaller than 1%. The calcium imaging data was analyzed using an algorithm designed in "R" (versions 3.6.2, Lucent Technologies, USA), using a previously reported methodology.[22]

2.7 | Statistical analysis

Statistical analysis was performed in "R." Briefly, a "Shapiro-Wilk normality test" was used to assess whether the data was normally distributed; a "Levene's test" was performed to evaluate the homogeneity of variances across groups. If the data was normally distributed and the variance across groups was homogeneous ("Shapiro–Wilk" and "Levene's test" both $p > 0.1$), "independent samples *t*-test" (between two groups) or "ANOVA + Tukey" (among more than two groups) was used to evaluate the statistical significance of differences between/among groups. This statistical method was used to analyze data of IVD cell viability and neuron subtype proportion.

IVDs from the same animal were assigned to overloaded and control groups. One IVD in the overloaded group was matched with another IVD in the control group if they were from the same animal. The groups were compared within the matched pairs to reduce the confounding effect of donor variation. Namely, the "paired *t*-test" was used to statistically analyze data of peak frequency and peak height of calcium flickering.

The specific statistical method and "*p* values" for each experiment were summarized in Table S2. In the figures presenting the data, each data point represents the average value of an IVD donor, and "*n*" value refers to the number of IVD donors.

3 | RESULTS

3.1 | IVD loading deformity monitoring

The real-time IVD deformities (strain) in response to loading (stress) were recorded (10 Hz) in the bioreactors. In the static loading regime, the FC loaded deformity was 10.6% on day 1 and was decreased to 7% on day 5. From day 5 to day 7, IVD deformity under FC loading remained at the minimum level of 7% (Figure 3A). The deformity of IVD in the FC group is composed with a fast elastic phase and a slow creep phase (Figure 3B). This 2-phase deformity of IVD has been described in a former study.[25] In the displacement-controlled group (DC), the IVD height was maintained as measured on day 0 (Figure 3A). The loading pressure required to maintain IVD height in DC group was recorded to be 0.02 MPa. Although the experimental setup in DC group was "displacement control," the pressure applied was consistently at 0.02 MPa on each day. Thus, DC group can be interpreted as a "mild force control" with a smaller pressure (0.02 MPa for DC compared to 0.2 MPa for FC).

In the dynamic loading regime, the high-frequency-intensity loading (DL group) resulted in a higher overall deformity each day (Figure 4A), but

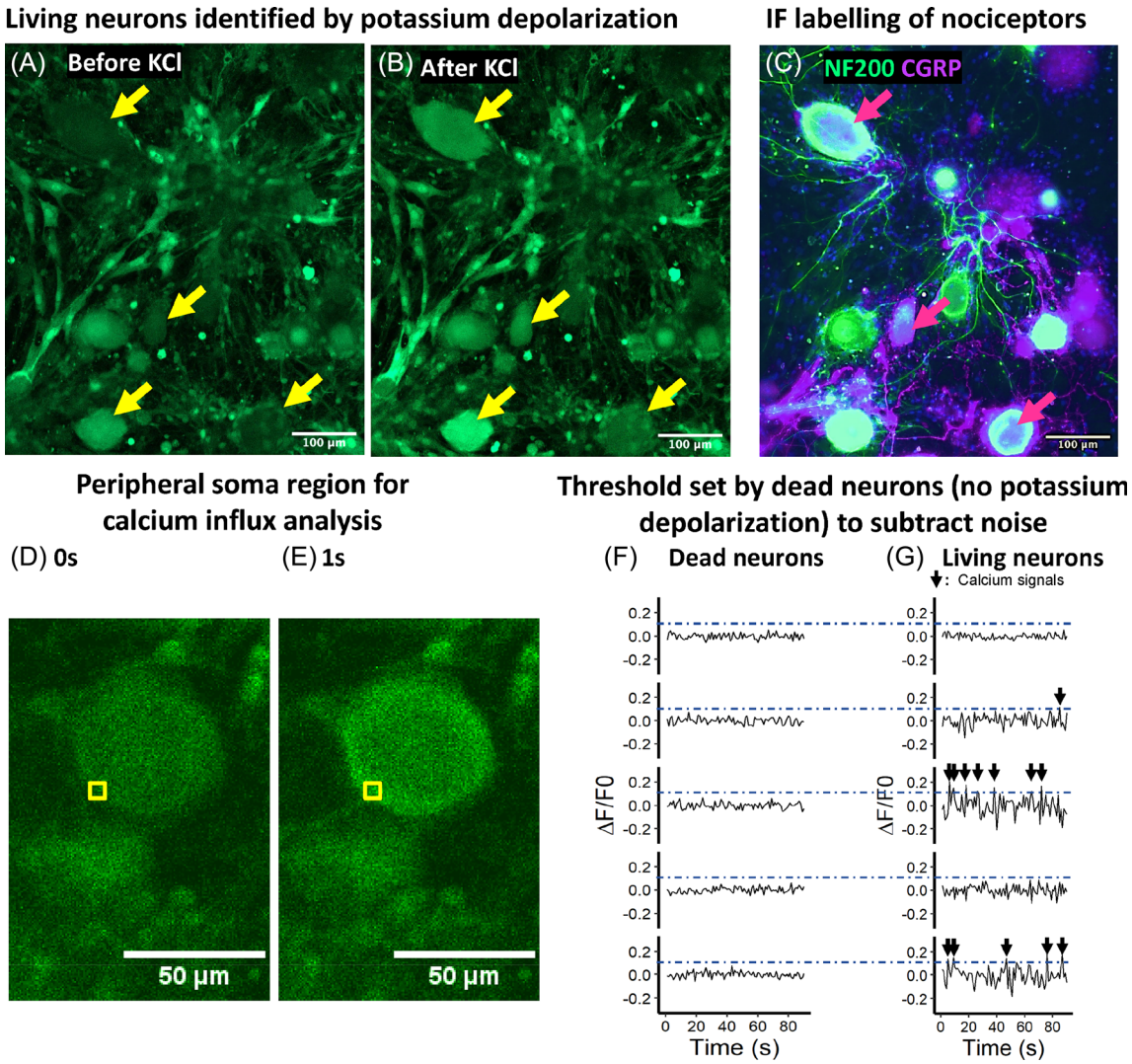

FIGURE 2 Methods for calcium imaging data analysis. (A,B) Only living neurons depolarize after adding potassium chloride (KCl 50 mM) (living neurons are indicated by yellow arrows). Dead neurons are without KCl-induced depolarization. (C) Nociceptors were labeled by CGRP immunofluorescent staining. (D,E) Regions of interest (ROIs, indicated by yellow squares) were selected at the peripheral regions of neuronal cell bodies. A calcium flickering in the subsurface space can be observed. (F,G) Fluorescence oscillations in dead neurons (left) were used to set a threshold (blue dash lines) to subtract noise.

a lower inter-peak deformity compared to the lower frequency-intensity loading (PL group) (Figure 4B). This lower inter-peak deformity in DL group can be explained by the viscoelastic property of IVD. The IVD undergoes creep and the deformity takes a certain amount of time.[25] The daily dynamic loadings caused the same amount of IVD deformity from day 1 to day 5 (always 20% for PL and 30% for DL) (Figure 4A).

3.2 | Viability of inner annulus fibrosus cells was decreased by force-controlled loading relative to displacement-controlled loading

Besides unrestorable IVD height loss, FC loading also influenced IVD cell viability. FC loading decreased the cell viability by 12.1% and 4.2% in inner AF (iAF) and NP regions of IVD, respectively, relative to DC loading (Figure 5A–D,G). No significant difference of IVD cell viability could be detected comparing PL with DL loadings (Figure 5H–N). Outer AF (oAF) cell viability was not influenced by any of the loading regimes (Figure 5E–G, L–N).

IVD degeneration is also characterized by altered gene expression and metabolic change of extracellular matrix. We found that 7 days of FC loading upregulated the expression of interleukin-6 (IL-6) and matrix metalloproteinase 13 (MMP13) in iAF and NP region of IVD relative to DC loading (Figure S2 in supporting information 2). Besides, the influences of different static and dynamic loadings on IVD gene expression at protein levels and IVD histology have been systematically characterized in other studies.[26–28]

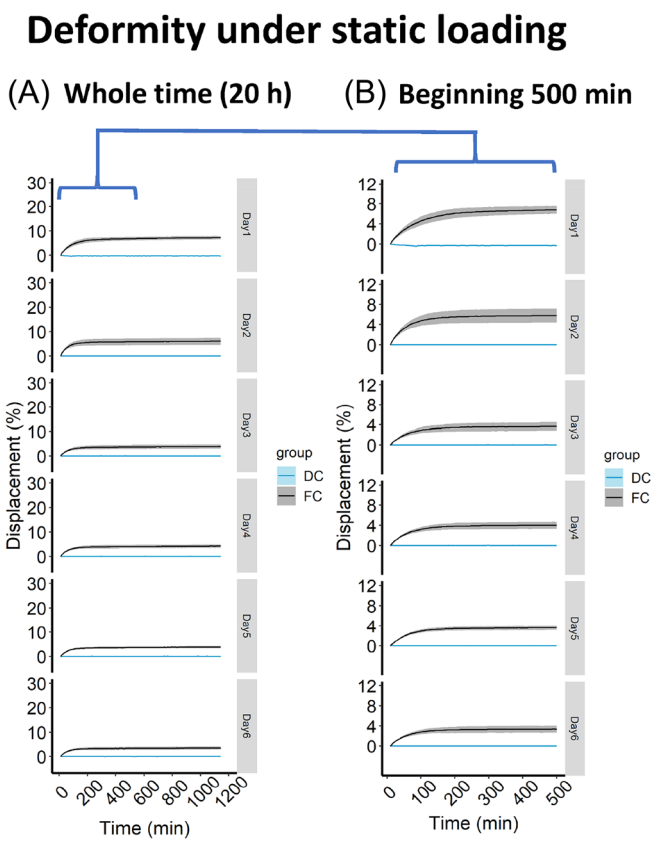

FIGURE 3 Deformity of IVD under static loading regime. (A) IVD deformity under 20 h of static loading. (B) IVD deformity of the first 500 min under static loading. DC, displacement-controlled static loading; FC, force-controlled static loading. Strata displays the level of standard errors, $n = 3$ donors.

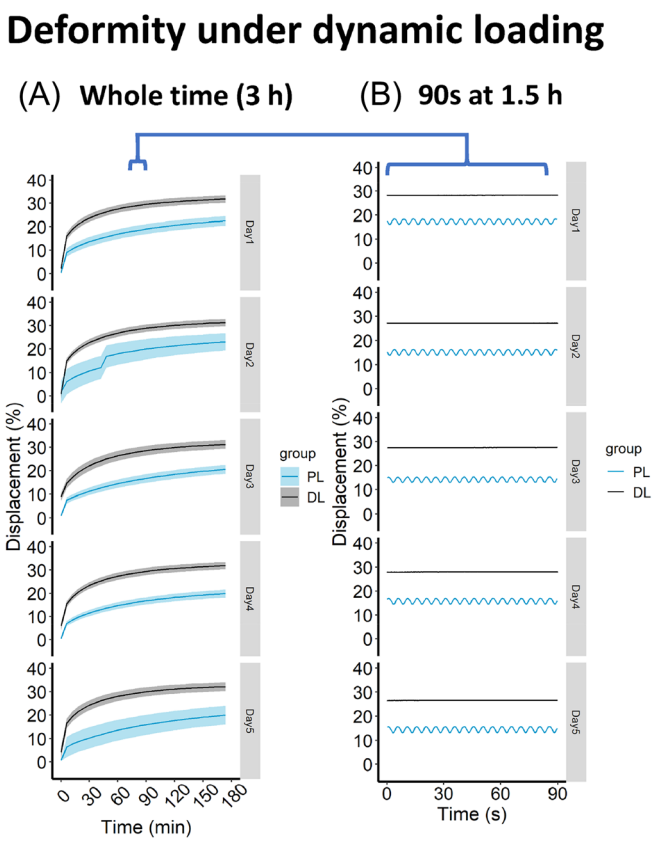

FIGURE 4 Deformity of IVD under dynamic loading regime. (A) IVD deformity under 3 h of dynamic loading. (B) To show the inter-peak deformity under dynamic loading, 90 s of real-time deformity are sampled in the middle of dynamic loading (at 1.5 h). DL, degenerative dynamic loading; PL, physiological dynamic loading. Strata displays the level of standard errors, $n = 3$ donors. "B" is based on one representative donor.

3.3 | Characterization of CGRP(+) nociceptors

CGRP is a well-known marker to label nociceptors in different species.[29] In this study, immunofluorescence of CGRP showed 3 DRG neuronal subpopulations: CGRP(+)NF200(−), CGRP(+)NF200(+) and CGRP(−)NF200(−) (Figure 6A,B). In the bovine DRG culture, the CGRP(+)NF200(−) nociceptors displayed smaller soma size compared to the CGRP(+)NF200(+) neurons and CGRP(−)NF200(+) neurons (Figure 6B). Nevertheless, since there is significant overlap among their distribution, CGRP(+)NF200(−) neurons cannot be distinguished from other neuronal populations solely by their size. Following the IVD conditioned medium stimulation, proportions of different neuronal subpopulations were not significantly changed suggesting no identifiable phenotype switch (Figure 6C–H).

3.4 | Force-controlled static loading on IVD increased calcium flickering frequency in CGRP(+) nociceptors

Following IVD CM stimulation, calcium imaging combined with immunofluorescence was performed to evaluate the activation of CGRP(+) nociceptors. The CM from the FC loaded IVDs induced significantly higher frequency of subsurface calcium flickering in CGRP(+) nociceptors compared to the DC control IVDs (Figure 7A–C). The subsurface calcium flickering frequency was seven calcium peaks per 100 s in FC group and 3 peaks per 100 s in DC group (Figure 7C). Data in all the IVD donors was showing the same trend (Figure 7C). The subsurface calcium flickering peak height was not found to be different between groups (Figure 7D).

3.5 | High-frequency-intensity dynamic loading of IVD increased calcium flickering frequency in CGRP (+) nociceptors

In terms of dynamic loading regimes, CM from high-frequency-intensity loaded IVD (DL group) elevated the frequency of subsurface calcium flickering in the CGRP(+) nociceptors compared to the lower-frequency-intensive loaded IVD counterpart (PL group) (Figure 7E–G). The subsurface calcium flickering frequency was seven peaks per 100 s in DL group and four peaks per 100 s in PL group. The same trend was observed in all the IVD donors (Figure 7G). The

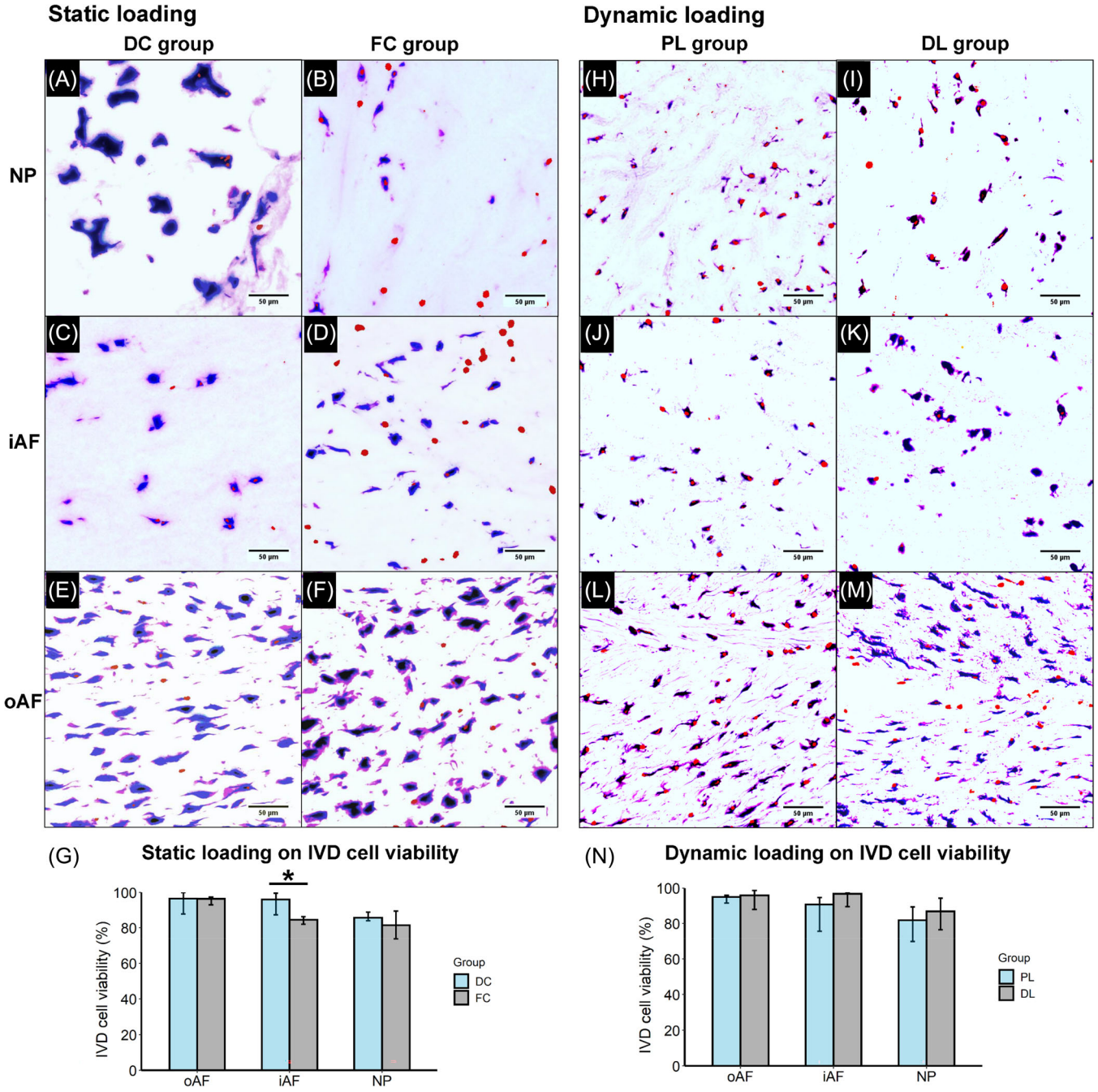

FIGURE 5 LDH and ethidium homodimer-1 staining of cryosections to study the influence of static and dynamic loadings on IVD cell viability. Representative microscopic images from static loaded (A–F) and dynamic loaded (H–M) IVDs in different regions. The red channel was adjusted for better visualization. (G,N) Quantification of the viability of static loaded IVD and dynamic loaded IVD, respectively. For G and N, data is shown as median ± 95% confident intervals. *$p < 0.05$.

subsurface calcium flickering peak height was not found to be significantly different between PL and DL groups (Figure 7H).

4 | DISCUSSION

The main goal of our study is to investigate how IVD overloading influences the IVD-nociceptor communication. We found that the frequency of calcium flickering in CGRP(+) nociceptors was enhanced by intensive IVD loading. This effect was observed in both IVD-narrowing static loading and high-frequency-intensity dynamic loadings compared to displacement-controlled and lower-frequency-intensity loadings, respectively. Much evidence showed that the neuronal calcium flickering couples with neuronal discharge.[14,30,31] Calcium flickering recorded using calcium imaging is commonly used to characterize ectopic discharge in neurons.[32] The

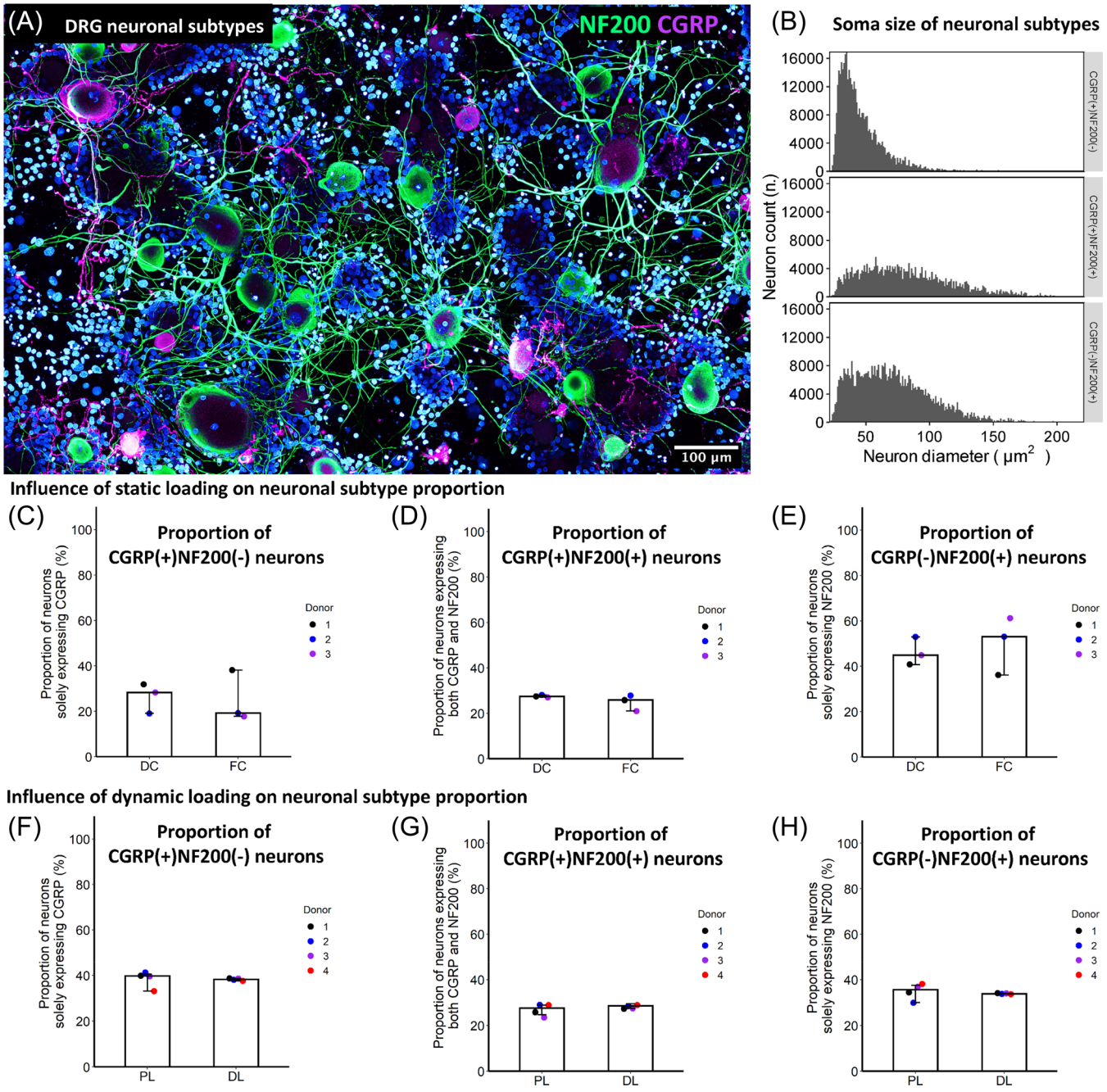

FIGURE 6 Characterization of bovine DRG neuronal subtypes. (A) A representative immunofluorescent image showing NF200 and CGRP labeled neurons. (B) Neuronal size distribution in different subtypes. (C–H) Dynamic or static loading on IVD does not significantly influence proportions of different neuronal subtype. Plots display median level ± 95% confident intervals. For (C–H), data points represent different IVD donors. Data are pooled from two DRG donors for either static or cyclic loading studies, respectively (four DRG donors overall).

calcium influx and the "calcium induced calcium release" from endoplasmic reticulum are both directly triggered by and in synergy with the neuronal excitation.[16] Therefore, our results may imply a role of IVD mechanical loading on ectopic discharge of nociceptors.

This IVD-nociceptor communication is demonstrated in our study by the IVD organ and primary DRG culture system. Nevertheless, we are aware that the complexity of chronic pain exceeds the sole excitation of nociceptors. The role of the central nervous system has not been included in the model. Moreover, chronic LBP is associated with numerous other mechanisms including immunology responses, genetic predisposition, behavioral and environmental factors, emotional state, beliefs and expectation and social system.[33] Additionally, clinical discogenic pain development usually takes years, but in our study, the IVD CM were collected to stimulate nociceptors only after 5 days of IVD loading. Our organ culture system cannot recapitulate the full picture of chronic discogenic pain but may help in

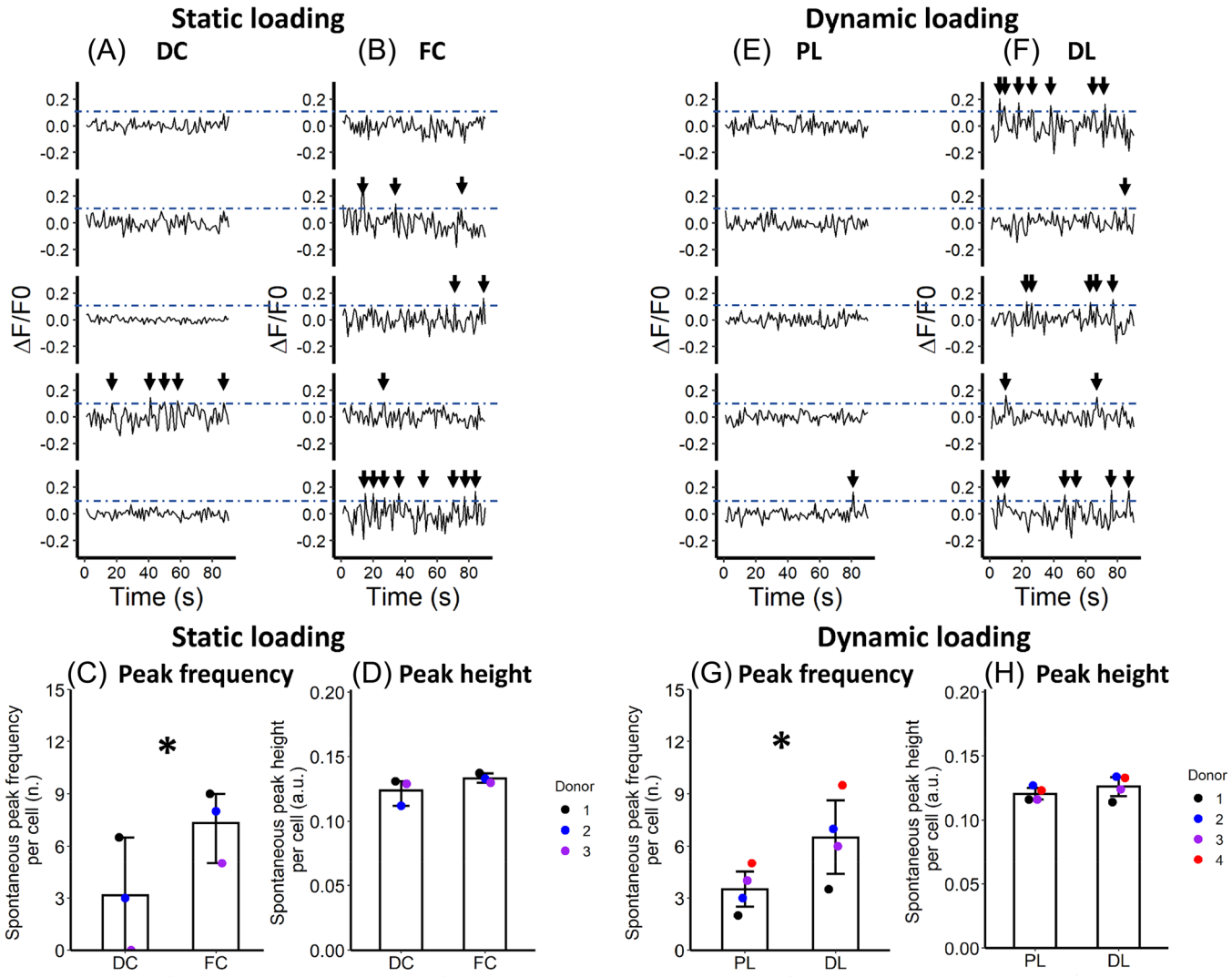

FIGURE 7 The influence of IVD loading regimes on the subsurface calcium flickering signals in bovine nociceptors. (A–D) High static force-controlled loading (FC) is compared with displacement-controlled loading (DC). (E–H) Degenerative dynamic loading with high frequency and intensity (DL) is compared with lower-frequency-intensity physiological loading (PL). For A,B and E,F, the normalized fluorescent curves are from five representative nociceptors. For C,D and G,H, data points represent different IVD donors. *$p < 0.05$. Mean levels are displayed with 95% confident interval.

understanding the regional and temporal IVD-nociceptor communicating mechanism which at least partly contributes to the development of chronic LBP.

Multiple mechanisms may underly the IVD-nociceptor communication. Molecules released by the IVD may cause a higher activation of nociceptors. Potential molecules include pro-inflammatory cytokines (e.g., IL-6,[34] IL-8[35] and Prostaglandin E2 [PGE2][36]), neurotrophins (e.g., nerve growth factor [NGF][37] and brain derived neurotrophic factor [BDNF][38]) and extracellular matrix fragments.[39] Also, nerve fibers growing deeply in the IVD[11] may be directly exposed to the stimulus from IVD loadings. Furthermore, IVD may influence nociceptors by depriving nutrients and accumulating metabolites, causing a low glucose, hypoxic and acidic environment which can lead to nociceptor sensitization.[24] In Supporting information 4, IVD CM were not inducing a higher nociceptor calcium flickering compared to fresh medium in a nociceptor cell line model (Figure S4). Also, primary bovine nociceptors stimulated by IVD CM displayed potassium induced depolarization, which indicates their viability. The nutrient consumption by IVD organ culture did not seem to harm nociceptors and induce their sensitization.

DRG neurons have complex subtypes. Recent single cell sequencing analysis predicts two types of neurons responsible for chronic pain. They are the "mechano-heat C-nociceptors (PEP1)" and the "nonpeptidergic nociceptor subtype 2 (NP2)".[40] CGRP is a well-known label of PEP1 nociceptors and has been shown to be a conserved molecular feature comparing mouse and rhesus macaques.[40] We labeled PEP1 nociceptors using CGRP in our DRG culture not only for their known roles in pain, but also because nerve fibers in the pain-producing IVD are found to be CGRP(+).[11,41] NP2 nociceptors have not been detected in the clinical IVD histology and were thus

not characterized in our model. However, it may be interesting to characterize NP2 nociceptors in future IVD-related studies. Similarly, IVD is also composed by different cell types. Whether these different cell types respond to overloading and communicate with nociceptor differently needs to be characterized in the future.

The IVD organ culture system has been well-established to study the role of mechanical loading on IVD degeneration. Using this organ culture system, it has been proved that mechanical loading plays a fundamental role for the regulation of IVD mechanical properties,[42] matrix homeostasis[26] and pro/anti-inflammatory gene expression.[27] These findings are systematically reviewed elsewhere.[6,43]

In former IVD organ culture studies, both free swelling[44] and static loading conditions (0.2 MPa)[7] have been used to maintain IVD following dynamic loading. These free swelling or static loading conditions after the dynamic loadings recapitulate the resting phase in a lying down position. However, the knowledge of in vivo IVD loading conditions in lying down position is limited. Our data (Supporting information 3) showed that even mild static loading at 0.02 MPa caused IVD degeneration compared to free swelling. We found that 7 days of 0.02 MPa static loading (20 h/day) induced higher cell death in the NP region and an upregulated IL-6 expression in outer AF region compared to the same duration of free-swelling culture (Figure S3). Notice that the 0.02 MPa loading was applied to keep the IVD height measured immediately after IVD harvesting. This height might be different to the in vivo physiological IVD height. In vivo characterization of IVD loading and deformity is needed to understand the physiological conditions for IVD organ culture models.

In vitro and ex vivo models are frequently questioned as they cannot totally recapitulate the in vivo situation. Indeed, an in vitro model cannot percept pain. Yet, it is still useful in studying specific pain-associated pathophysiology with higher access to experimental manipulation and evaluation. In the organ culture system, the IVD mechanical loading is easier to control and calcium flickering of neurons is less demanding to observe. Also, we used organs and tissues from large animals which are considered to be more similar to human as compared to studies performed using rodents.[45] The large animal materials from the abattoir also open a new strategy of reducing and replacing animal use in line with 3R principles.

5 | CONCLUSIONS AND PERSPECTIVES

In the static loading regime, force-controlled loading leads to an increased IVD cell death compared to displacement-controlled loading. Both static and dynamic IVD overloadings elevated calcium flickering in the subsurface space of CGRP(+) nociceptors compared to their mild loading counterparts, which indicates a higher ectopic discharge in these nociceptors.

To understand the mechanism of discogenic pain, the influence of loading on IVD-nociceptor communication is important in addition to assessment of IVD degeneration. The next challenge is to understand the molecular mechanisms of this IVD-nociceptor communication. Our presented model may help in discovery of novel molecular targets for clinical discogenic pain treatment and reduce the reliance on animal models.

AUTHOR CONTRIBUTIONS

Marianna Peroglio, Junxuan Ma and Mauro Alini contributed to the conception and design of the study. Jan Gewiess, Janick Eglauf, Junxuan Ma and Astrid Soubrier performed the experiments, data acquisition and analysis. Marianna Peroglio, Sibylle Grad, Junxuan Ma and Mauro Alini contributed to grant application and project management. Junxuan Ma wrote the manuscript. All authors contributed to revise the manuscript.

ACKNOWLEDGMENTS

The authors would like to gratefully acknowledge N. Goudsouzian, D. Nehrbass and M. Bluvol for their assistance with histological preparations and R. Peter and Fleischzentrum Klosters Davos AG for the support and supply of the bovine tails and DRG tissue. The study was funded by the AO Foundation.

CONFLICT OF INTEREST STATEMENT

Sibylle Grad and Marianna Peroglio are Editorial Board members and Mauro Alini is an Editor of JOR Spine, and all are co-authors of this article. To minimize bias, they were exclude from all editorial decision-making related to the acceptance of this article for publication. [Correction added on 22 June 2023, after first online publication: Conflict of Interest statement was revised]

ORCID

Sibylle Grad https://orcid.org/0000-0001-9552-3653
Mauro Alini https://orcid.org/0000-0002-0262-1412
Junxuan Ma https://orcid.org/0000-0001-8923-9832

REFERENCES

1. Disease GBD, Injury I, Prevalence C. Global, regional, and national incidence, prevalence, and years lived with disability for 310 diseases and injuries, 1990–2015: a systematic analysis for the Global Burden of Disease Study 2015. *Lancet*. 2016;*388*(10053):1545-1602.
2. DePalma MJ, Ketchum JM, Saullo T. What is the source of chronic low back pain and does age play a role? *Pain Med*. 2011;*12*(2):224-233.
3. Oliveira CB, Pinheiro MB, Teixeira RJ, et al. Physical activity as a prognostic factor of pain intensity and disability in patients with low back pain: a systematic review. *Eur J Pain*. 2019;*23*(7):1251-1263.
4. Bakker EW, Verhagen AP, van Trijffel E, Lucas C, Koes BW. Spinal mechanical load as a risk factor for low back pain: a systematic review of prospective cohort studies. *Spine (Phila Pa 1976)*. 2009;*34*(8):E281-E293.
5. Battié MC, Videman T, Kaprio J, et al. The twin spine study: Contributions to a changing view of disc degeneration. *Spine J*. 2009;*9*(1):47-59.
6. Gantenbein B, Illien-Jünger S, Chan S, et al. Organ culture bioreactors—platforms to study human intervertebral disc degeneration and regenerative therapy. *Curr Stem Cell Res Ther*. 2015;*10*(4):339-352.
7. Illien-Jünger S, Grad S, Lezuo P, et al. The combined effects of limited nutrition and high-frequency loading on intervertebral discs with endplates. *Spine (Phila Pa 1976)*. 2010;*35*(19):1744-1752.
8. Puopolo M, Mendell LM. Nociceptors: the gateway to pain. *Reference Module in Neuroscience and Biobehavioral Psychology*. Elsevier; 2017.
9. Reichling DB, Levine JD. Critical role of nociceptor plasticity in chronic pain. *Trends Neurosci*. 2009;*32*(12):611-618.

10. Aguirre J, Del Moral A, Cobo I, Borgeat A, Blumenthal S. The role of continuous peripheral nerve blocks. *Anesthesiol Res Pract*. 2012;*2012*:560879.
11. Freemont AJ, Peacock TE, Goupille P, Hoyland JA, O'Brien J, Jayson MIV. Nerve ingrowth into diseased intervertebral disc in chronic back pain. *Lancet*. 1997;*350*(9072):178-181.
12. Miyagi M, Millecamps M, Danco AT, Ohtori S, Takahashi K, Stone LS. ISSLS prize winner: increased innervation and sensory nervous system plasticity in a mouse model of low back pain due to intervertebral disc degeneration. *Spine (Phila Pa 1976)*. 2014;*39*(17):1345-1354.
13. Serra J, Bostock H, Solà R, et al. Microneurographic identification of spontaneous activity in C-nociceptors in neuropathic pain states in humans and rats. *Pain*. 2012;*153*(1):42-55.
14. Sasaki T, Takahashi N, Matsuki N, Ikegaya Y. Fast and accurate detection of action potentials from somatic calcium fluctuations. *J Neurophysiol*. 2008;*100*(3):1668-1676.
15. Ladewig T, Keller BU. Simultaneous patch-clamp recording and calcium imaging in a rhythmically active neuronal network in the brainstem slice preparation from mouse. *Pflugers Arch*. 2000;*440*(2):322-332.
16. Ouyang K, Zheng H, Qin X, et al. Ca^{2+} sparks and secretion in dorsal root ganglion neurons. *Proc Natl Acad Sci U S A*. 2005;*102*(34):12259-12264.
17. Billy GG, Lemieux SK, Chow MX. Changes in lumbar disk morphology associated with prolonged sitting assessed by magnetic resonance imaging. *PM R*. 2014;*6*(9):790-795.
18. Pope MH, Kaigle AM, Magnusson M, Broman H, Hansson T. Intervertebral motion during vibration. *Proc Inst Mech Eng Pt H J Eng Med*. 1991;*205*(1):39-44.
19. AO Research Institute Davos, Pattappa G, Peroglio M, et al. CCL5/RANTES is a key chemoattractant released by degenerative intervertebral discs in organ culture. *Eur Cell Mater*. 2014;*27*:124-136. discussion 136.
20. Jahn K, Stoddart MJ. Viability assessment of osteocytes using histological lactate dehydrogenase activity staining on human cancellous bone sections. *Methods Mol Biol*. 2011;*740*:141-148.
21. AO Research Institute, Stoddart MJ, Furlong PI, Simpson A, Davies CM, Richards RG. A comparison of non-radioactive methods for assessing viability in ex vivo cultured cancellous bone: technical note. *Eur Cell Mater*. 2006;*12*:16-25. discussion 16–25.
22. Ma J, Patil V, Pandit A, et al. In vitro model to investigate communication between dorsal root ganglion and spinal cord glia. *Int J Mol Sci*. 2021;*22*(18):9725.
23. Andersen PL, Doucette JR, Nazarali AJ. A novel method of eliminating non-neuronal proliferating cells from cultures of mouse dorsal root ganglia. *Cell Mol Neurobiol*. 2003;*23*(2):205-210.
24. Ma J, Stefanoska D, Grad S, Alini M, Peroglio M. Direct and intervertebral disc-mediated sensitization of dorsal root ganglion neurons by hypoxia and low pH. *Neurospine*. 2020;*17*(1):42-59.
25. Keller TS, Spengler DM, Hansson TH. Mechanical behavior of the human lumbar spine. I. Creep analysis during static compressive loading. *J Orthop Res*. 1987;*5*(4):467-478.
26. Chan SC, Walser J, Käppeli P, Shamsollahi MJ, Ferguson SJ, Gantenbein-Ritter B. Region specific response of intervertebral disc cells to complex dynamic loading: an organ culture study using a dynamic torsion-compression bioreactor. *PLoS One*. 2013;*8*(8):e72489.
27. Navone SE, Peroglio M, Guarnaccia L, et al. Mechanical loading of intervertebral disc modulates microglia proliferation, activation, and chemotaxis. *Osteoarthr Cartil*. 2018;*26*(7):978-987.
28. Paul CP, Schoorl T, Zuiderbaan HA, et al. Dynamic and static overloading induce early degenerative processes in caprine lumbar intervertebral discs. *PLoS One*. 2013;*8*(4):e62411.
29. Shiers S, Klein RM, Price TJ. Quantitative differences in neuronal subpopulations between mouse and human dorsal root ganglia demonstrated with RNAscope in situ hybridization. *Pain*. 2020;*161*(10):2410-2424.
30. Kleindienst T, Lohmann C. Simultaneous patch-clamping and calcium imaging in developing dendrites. *Cold Spring Harb Protoc*. 2014;*2014*(3):324-328.
31. Nguyen C, Upadhyay H, Murphy M, et al. Simultaneous voltage and calcium imaging and optogenetic stimulation with high sensitivity and a wide field of view. *Biomed Opt Express*. 2019;*10*(2):789-806.
32. Anderson M, Zheng Q, Dong X. Investigation of pain mechanisms by calcium imaging approaches. *Neurosci Bull*. 2018;*34*(1):194-199.
33. Vlaeyen JWS, Maher CG, Wiech K, et al. Low back pain. *Nat Rev Dis Primers*. 2018;*4*(1):52.
34. Zhou YQ, Liu Z, Liu ZH, et al. Interleukin-6: an emerging regulator of pathological pain. *J Neuroinflammation*. 2016;*13*(1):141.
35. Krock E, Millecamps M, Anderson KM, et al. Interleukin-8 as a therapeutic target for chronic low back pain: upregulation in human cerebrospinal fluid and pre-clinical validation with chronic reparixin in the SPARC-null mouse model. *EBioMedicine*. 2019;*43*:487-500.
36. van Dijk B, Potier E, Licht R, Creemers L, Ito K. The effect of a cyclooxygenase 2 inhibitor on early degenerated human nucleus pulposus explants. *Global Spine J*. 2014;*4*(1):33-40.
37. Abe Y, Akeda K, An HS, et al. Proinflammatory cytokines stimulate the expression of nerve growth factor by human intervertebral disc cells. *Spine (Phila Pa 1976)*. 2007;*32*(6):635-642.
38. Gruber HE, Ingram JA, Hoelscher G, Zinchenko N, Norton HJ, Hanley EN Jr. Brain-derived neurotrophic factor and its receptor in the human and the sand rat intervertebral disc. *Arthritis Res Ther*. 2008;*10*(4):R82.
39. Krock E, Rosenzweig DH, Currie JB, Bisson DG, Ouellet JA, Haglund L. Toll-like receptor activation induces degeneration of human intervertebral discs. *Sci Rep*. 2017;*7*(1):17184.
40. Kupari J, Usoskin D, Parisien M, et al. Single cell transcriptomics of primate sensory neurons identifies cell types associated with chronic pain. *Nat Commun*. 2021;*12*(1):1510.
41. Aoki Y, Ohtori S, Takahashi K, et al. Expression and co-expression of VR1, CGRP, and IB4-binding glycoprotein in dorsal root ganglion neurons in rats: differences between the disc afferents and the cutaneous afferents. *Spine (Phila Pa 1976)*. 2005;*30*(13):1496-1500.
42. Wang Y, Chen HB, Zhang L, Zhang LY, Liu JC, Wang ZG. Influence of degenerative changes of intervertebral disc on its material properties and pathology. *Chin J Traumatol*. 2012;*15*(2):67-76.
43. Chan SC, Ferguson SJ, Gantenbein-Ritter B. The effects of dynamic loading on the intervertebral disc. *Eur Spine J*. 2011;*20*(11):1796-1812.
44. Lang G, Liu Y, Geries J, et al. An intervertebral disc whole organ culture system to investigate proinflammatory and degenerative disc disease condition. *J Tissue Eng Regen Med*. 2018;*12*(4):e2051-e2061.
45. Casal M, Haskins M. Large animal models and gene therapy. *Eur J Hum Genet*. 2006;*14*(3):266-272.

SUPPORTING INFORMATION

Additional supporting information can be found online in the Supporting Information section at the end of this article.

How to cite this article: Gewiess, J., Eglauf, J., Soubrier, A., Grad, S., Alini, M., Peroglio, M., & Ma, J. (2023). The influence of intervertebral disc overloading on nociceptor calcium flickering. *JOR Spine*, *6*(3), e1267. https://doi.org/10.1002/jsp2.1267